

Approval Talk [HIG-23-005]

“Search for rare decays of the Higgs boson into a photon and a ρ^0 , ϕ or K^{*0} meson”

R. Covarelli¹ M. Pelliccioni¹ G. Umoret¹
M. D'Alfonso² G. Gomez Ceballos² C. Paus² K. Yoon²

¹Politecnico di Torino, Turin, Italy

²Massachusetts Institute of Technology, Cambridge, U.S.

March 19, 2024

About this analysis

FIX! add paper front page

HIG-23-005

Collaboration

- Collaboration of **MIT** and **Torino** groups, targeting different Higgs production categories.

Conveners

- **ARC**: Anadi Canepa (chair), Stefan Spanier, Jian Wang, Angelo Giacomo Zecchinelli
- **CCLE**: Christoph Maria Ernst Paus

Documentation

- Relevant links: [CADI](#), [TWiki](#)
- Latest ANs (two individual + one combined):
[AN-22-004](#) (MIT, v9), [AN-22-067](#) (Torino, v10), and [AN-23-004](#) (combined, v7)

Introduction

Higgs coupling with light quarks (u, d, s)

- Suppressed couplings and large QCD background hamper direct searches.
- Class of decays suggested $H \rightarrow M\gamma$, where M is a light-quark meson.
- *In this analysis, $M = \phi, \rho^0, K^{*0}$ are considered.*

Channel	Coupling	SM $\mathcal{BR}(H \rightarrow M\gamma)$
$H \rightarrow \phi\gamma$	s	$(1.68 \pm 0.08) \times 10^{-5}$ [1]
$H \rightarrow \rho^0\gamma$	u, d	$(2.31 \pm 0.11) \times 10^{-6}$ [1]
$H \rightarrow K^{*0}\gamma$	$d\&s$ (flavor-changing)	(Only available for $H \rightarrow d\bar{s} + \bar{d}s$) 1.19×10^{-11} [2]

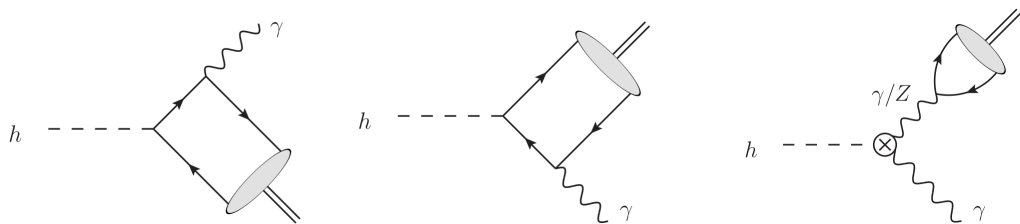
Table 1: $H \rightarrow M\gamma$ channels considered in this analysis with their respective couplings and predicted branching ratios.

Motivations

$H \rightarrow M\gamma$

- **Direct contribution.** The Higgs couples via Yukawa coupling to the quarks, one of which radiates a photon.
- **Indirect contribution.** The off-shell γ^* or Z^* produced in $H \rightarrow \gamma\gamma^*, \gamma Z^*$ fragments into a meson.

Direct and indirect contributions interfere destructively. Due to light quark masses, direct contribution is smaller than indirect. *Direct contribution is sensitive to deviation from SM.* Branching ratios are typically $\mathcal{O}(10^{-5}\text{--}10^{-6})$.



(a) Direct contributions via Yukawa coupling to the light quarks.

(b) Indirect contribution via a virtual photon or Z boson.

Figure 1: Leading order Feynman diagrams to the $H \rightarrow M\gamma$ processes. Image taken from Fig. 2 of [1].

Flavor-conserving probes

- ϕ : s quark coupling (diagrams above)
- ρ^0 : u and d quark coupling

Flavor-changing probe

- K^{*0} : flavor-changing s and d quarks via weak interaction (diagrams below)

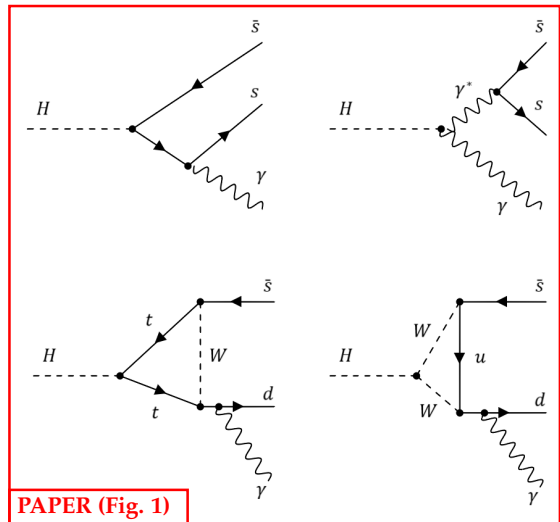


Figure 2: Feynman diagrams showing the different Higgs boson decay mechanisms into a photon and a light meson (top: ϕ meson; bottom: K^{*0} meson).

Analysis Strategy

Analysis Strategy

- **Final states**

1. High energy **photon**.
2. High energy **di-track** from meson.



$$\mathcal{BR}(\rho^0 \rightarrow \pi^+ \pi^-) \sim= 100\%$$



$$\mathcal{BR}(\phi \rightarrow K^+ K^-) \sim 49\%$$



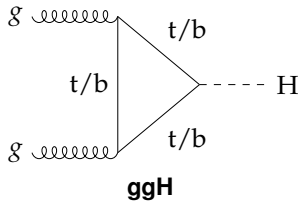
$$\mathcal{BR}(K^{*0} \rightarrow K^\pm \pi^\mp) \sim 100\%$$

Figure 3: Di-track systems for the different mesons considered in this analysis.

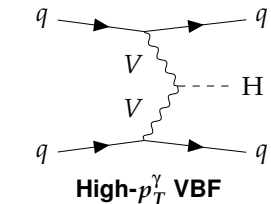
3. Signal events extracted from **photon & di-track invariant mass spectrum**.

Analysis Strategy

- Higgs Production Categories



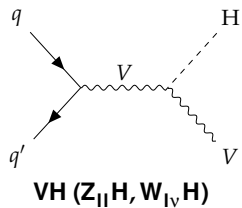
- No e/μ.



- $p_T^\gamma > 75 \text{ GeV}$.
- No e/μ

Low- p_T^γ VBF

- $40 < p_T^\gamma < 75 \text{ GeV}$.
- No e/μ



VH ($Z_{ll}H, W_{l\nu}H$)

- At least one e/μ.
- Also included is $t\bar{t}H$, accounting for $\sim 30\%$.

Triggers

- **High Level Triggers (HLT)**

Three types of triggers are employed.

Tau-like trigger

Photon + jets with τ -ID

→ **ggH, low- p_T^γ VBF**

- Photon $p_T^\gamma > 35$ GeV + tau-like jet $p_T^j > 35$ GeV.
- Tau-leg similar to isolated di-track system.
- Active during 2018.

VBF-dedicated trigger

High- p_T^γ photon + VBF-like jets

→ **high- p_T^γ VBF**

- Photon $p_T^\gamma > 35$ GeV + di-jet with large M_{jj} and $\Delta\eta_{jj}$.
- Active partly during 2016-17 and fully during 2018.

Leptonic trigger

Double or single lepton

→ **VH**

- Single or double-muon (electron) lowest p_T thresholds vary depending on year.
- To complement selection, triggers requiring a lepton and a photon is also used.

Triggers

- **High Level Triggers (HLT)**

	ggH	High- p_T^γ VBF	Low- p_T^γ VBF	VH
Triggers	tau-like	VBF-like	tau-like	single/di-muon single/di-electron muon+gamma
Luminosity (fb^{-1})	39.50 (2018)	28.2 (2016) 7.7 (2017) 60 (2018)	39.50 (2018)	138 (2016–2018)

- **HLT Efficiencies and Scale Factors**

Trigger efficiency **scale factor** defined as the ratio of data vs. MC efficiency.

$$SF = \frac{\epsilon_{\text{Data}}}{\epsilon_{\text{MC}}}$$

- **HLT Efficiencies and Scale Factors**

For the tau-like trigger, Data = Single Muon, MC = Drell-Yan. Photon-leg and tau-leg efficiencies measured separately, where

FIXME do I need these equations?

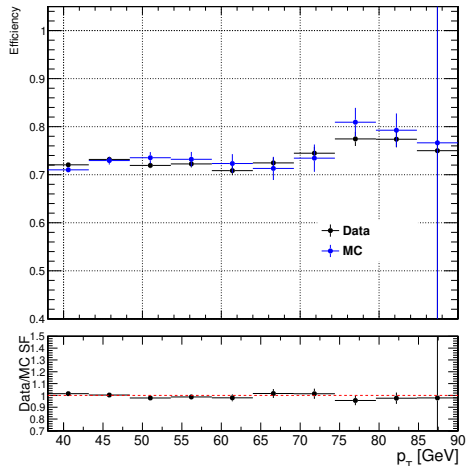
$$\epsilon_{\gamma}^{\text{HLT}} = \frac{\text{HLT_Mu17_Photon30} \wedge \text{offline selection} \wedge \text{HLT_IsoMu24}}{\text{offline selection} \wedge \text{HLT_IsoMu24}}$$

$$\epsilon_{\text{TwoProngs}}^{\text{HLT}} = \frac{\text{HLT_IsoMu24_TwoProngs35} \wedge \text{offline selection} \wedge \text{HLT_IsoMu24}}{\text{offline selection} \wedge \text{HLT_IsoMu24}}$$

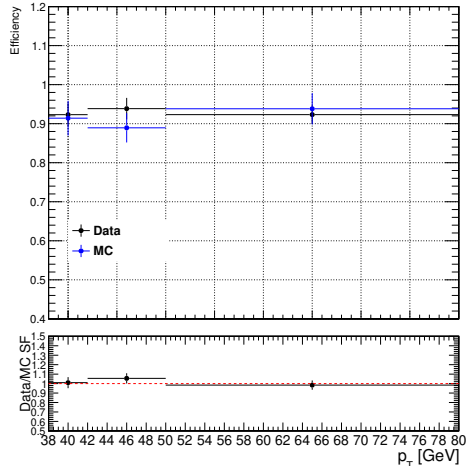
Triggers

- **HLT Efficiencies and Scale Factors**

Tau-like trigger efficiencies MC (blue) vs. Data (black).



(a) Tau-like trigger photon-leg efficiencies for MC and data.



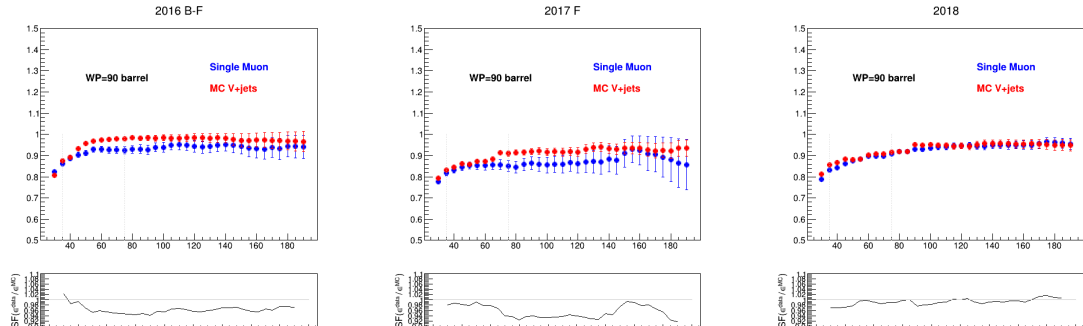
(b) Tau-like trigger tau-leg efficiencies for MC and data.

Figure 4: Photon-leg and tau-leg efficiencies of the tau-like trigger.

Triggers

- **HLT Efficiencies and Scale Factors**

VBF-dedicated trigger efficiencies MC (red) vs. Data (blue).



(a) VBF trigger photon-leg efficiencies for MC and data.

Figure 5: VBF-dedicated trigger photon-leg efficiencies for MC and data, shown for the $H \rightarrow p^0 \gamma$ channel in 2016 (top-left), 2017 (top-right), and 2018 (bottom).

Simulated Samples

Simulated Samples

- **MC Generation**

Gen-level: POWHEG (NLO) or MADGRAPH5_aMC@NLC (LO)

PDFs: NNPDF3.1 (NNLO)

Hadronization: PYTHIA 8.212

- SM processes considered in background simulation are γ , $W \rightarrow l\nu$, Drell-Yan $Z \rightarrow ll$ with jets, $t\bar{t}$, $W\gamma$, and $Z\gamma$.
- Cross sections for Higgs production: FIX! double check

Process	σ (fb)
ggH	48580
VBF	3782
$W_{l\nu}H$	471
$Z_{ll}H$	77

- **Signal Simulation**

Polarization reweighting of events.

Higgs is a scalar, and angular momentum conservation constrains the mesons to have transverse spin alignment in the $H \rightarrow M\gamma$ process. PYTHIA simulates unpolarized decay products. Therefore, signal events are reweighted by $(3/2) \sin^2 \theta$, where θ is the angle between positive track in meson rest frame and meson flight direction in lab frame.

FIX! Which plot to include?

Event Selection

Event Selection

- **Photon selection**

	ggH	High- p_T^γ VBF	Low- p_T^γ VBF	VH
p_T^γ [GeV]	> 38	> 75	$38 < p_T^\gamma < 75$	> 40
$ \eta^\gamma $	< 2.1	< 1.4	< 2.1	< 2.5
γ -ID signal eff.	80%	90%	80%	90%

Table 2: Photon selection criteria across different production categories.

- γ -ID signal eff. = MVA-based selection ID [3]
- p_T^γ cut based on trigger
- **FIX!** ggH & VH—**BUT PAPER IS NOT FIXED!**
- ggH/VBF: conversion veto, VH: pixel veto.
- Highest- p_T^γ photon chosen as candidate.

Event Selection

- **Di-track system reconstruction**

Track selection

- Originate from PV.
- Pass “high purity” criteria.

Meson definition

- Pair of oppositely charged tracks.
- $p_T > 5 \text{ GeV}$, $|\eta| < 2.5$.
- At least one track $p_T > 20 \text{ GeV}$.

Invariant mass

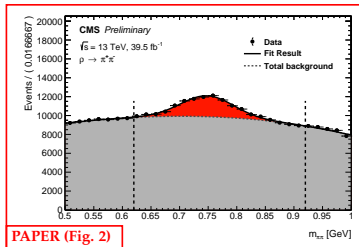
- Di-track system invariant **mass windows and sidebands** (next slide).
- $K^\pm\pi^\mp$ system: if both combinations exist, then the one closest to $m_{K^{*0}}$ is selected.
- Reject events where m_{KK} consistent with m_π and have higher p_T , vice versa.

Applies to all production categories.

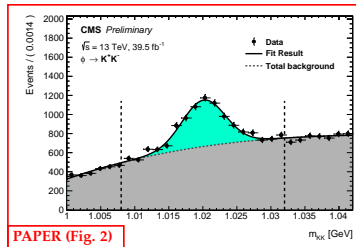
Event Selection

- **Di-track system reconstruction**

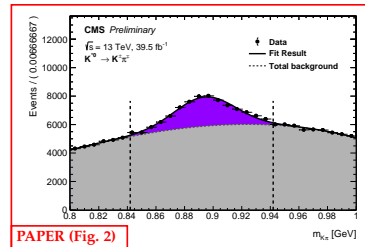
Mass windows applied to invariant mass of di-track system.



ρ^0 mass window: $0.62 < m_{\pi\pi} < 0.92 \text{ GeV}$
Sidebands: $0.50 < m_{\pi\pi} < 0.62 \text{ GeV}$
 $0.92 < m_{\pi\pi} < 1.00 \text{ GeV}$



ϕ mass window: $1.008 < m_{K^*K^*} < 1.032 \text{ GeV}$
Sidebands: $1.000 < m_{K^*K^*} < 1.008 \text{ GeV}$
 $1.032 < m_{K^*K^*} < 1.050 \text{ GeV}$



K^{*0} mass window: $0.84 < m_{K\pi} < 0.94 \text{ GeV}$
Sidebands: $0.80 < m_{K\pi} < 0.84 \text{ GeV}$
 $0.94 < m_{K\pi} < 1.00 \text{ GeV}$

Figure 6: Di-track mass distribution in selected events in data, for the ggH category of the analysis, $\rho^0 \gamma$ (left), $\phi \gamma$ (middle) and $K^{*0} \gamma$ (right) channels. Vertical dashed lines represent the signal mass region borders.

Fix! Answer ARC MAR 05 question 2.

Event Selection

- **Di-track system selection**

Define the relative **charged isolation** of the leading meson candidate,

$$I^{\text{trk}}(M) = \frac{p_T^M}{p_T^M + \sum_{\text{trk}} |p_T^{\text{trk}}|},$$

and the **neutral isolation** as

$$I^{\text{neu}}(M) = \frac{p_T^M}{p_T^M + \sum_{\text{neu}} |p_T^{\text{neu}}|}.$$

$\sum_{\text{trk/neu}} |p_T^{\text{trk/neu}}|$: sum of charged/neutral track p_T within $\Delta R = 0.3$ of meson candidate.

	ggH	High- p_T^γ VBF	Low- p_T^γ VBF	VH
p_T^M [GeV]	> 38	> 40	> 40	> 40
I_M^{trk}	> 0.9	> 0.9	> 0.9	> 0.8
I_M^{neu}	> 0.8	-	-	-

Table 3: Di-track system criteria across different production categories.

Event Selection

- Event tagging

	ggH	High- p_T^γ VBF	Low- p_T^γ VBF	VH
Event tagging	Meson candidate within a jet with $p_T^j > 40$ GeV, tracks with $\Delta R < 0.07$	2 jets with $p_T^j > 40$ GeV, $m_{jj} > 400$ GeV, $\eta_{jj} > 3$	2 jets with $p_T^j > 30, 20$ GeV, $m_{jj} > 300$ GeV, $\eta_{jj} > 3$	1 selected and isolated e/μ or 2 selected e/μ compatible with m_Z

Table 4: Event tagging selection criteria across different production categories.

Event Selection

Summary of Event Selection

Common selections				
2 "high-purity" tracks, opposite sign				
$ \eta^{\text{trk}} < 2.5, p_T^{\text{trk}1} > 20 \text{ GeV}, p_T^{\text{trk}2} > 5 \text{ GeV}, \eta^M < 2.1$				
M selection	$0.62 < m_{\pi\pi} < 0.92 \text{ GeV} (\rho^0) / 1.008 < m_{KK} < 1.032 \text{ GeV} (\phi) / 0.84 < m_{K\pi} < 0.94 \text{ GeV} (K^{*0})$			
Category	ggH	VBF high- p_T^γ	VBF low- p_T^γ	VH
Trigger	Photon + jet with τ -ID	high- p_T photon + VBF-like jets	Photon + jet with τ -ID	Double or single lepton
p_T^γ [GeV]	> 38	> 75	> 40 and < 75	> 40
$ \eta^\gamma $	< 2.5	< 1.4	< 2.1	< 2.5
γ -ID signal eff.	80%	90%	80/90%	90%
p_T^M [GeV]	> 38	> 30	> 38	> 38
$I^{\text{trk}}(M)$	> 0.9	> 0.9	> 0.9	> 0.8
$I^{\text{neu}}(M)$	> 0.8	-	-	-
Event tagging	Meson candidate within a jet with $p_T^j > 40$ GeV, tracks with $\Delta R < 0.07$	2 jets with $p_T^j > 40$ GeV	2 jets with $p_T^j > 30/20$ GeV	1 selected and isolated e/ μ or 2 selected e/ μ compatible with Z mass
BDT categories				
cat0	BDT > 0.55	BDT > 0.7	BDT > 0.7	-
cat1	$-0.4 < \text{BDT} < 0.55$	$-0.6 < \text{BDT} < 0.7$	$-0.6 < \text{BDT} < 0.7$	-
PAPER (Table 1)				

Figure 7: Summary of the event selections, including both common and category-specific selections.

MC/Data Background Comparison

FIX! todo

Multivariate Analysis Selection

- **Multivariate Analysis (MVA) Overview**

Motivation

Improvement of signal-to-background ratio in categories with backgrounds dominated by $\gamma + \text{jet}$ and multijet events. → **ggH, low- p_T^γ VBF**, and **high- p_T^γ VBF** categories.

Methodology

- BDT classifiers based on ROOT TMVA [4], optimized with the Gradient boosting method.
- Training and validation samples defined by **meson mass SR & sidebands**.
- Signal & Background events weighted by $1/(\sigma M/M)$, where

$$\frac{\sigma M}{M} = \sqrt{\left(\frac{\sigma M}{M}\right)_{\text{meson}}^2 + \left(\frac{\sigma E}{E}\right)_\gamma^2}$$

- BDT classification is further split into **two sub-categories** (“cat0” and “cat1”) based on optimized discriminator threshold values to improve upper limit results.

Multivariate Analysis Selection

- MVA Overview

Input variables:

	ggH	High- p_T^γ VBF	Low- p_T^γ VBF
Kinematics		$p_T^{M\gamma}$	$p_T^{M\gamma}$
	p_T^γ	p_T^γ	p_T^γ
	p_T^M	$p_T^M / m_{M\gamma}$	$p_T^M / m_{M\gamma}$
	η_M		
Meson Isolation	$I^{\text{trk}}(\text{trk}_1)$	$I^{\text{trk}}(\text{trk}_1)$	$I^{\text{trk}}(\text{trk}_1)$
Jet-related		M_{jj}	M_{jj}
		$\Delta\phi_{jj}$	$\Delta\phi_{jj}$
		z^*	z^*

Table 5: Input variables used for ggH and VBF categories.

z^* is the Zeppenfeld variable, defined as $z^* = |\eta_{M\gamma} - 0.5(\eta_{j1} + \eta_{j2})| / |\Delta\eta_{jj}|$.

- MVA: ggH category

- Training samples

Signal: MC-generated

Background: Data from meson mass sidebands.

- 4 input variables

p_T^γ	photon p_T
p_T^M	meson p_T
η_M	meson η
$I^{\text{trk}}(\text{trk}_1)$	leading-track charged isolation

- BDT sub-categories

cat0: BDT-score > 0.55, optimized for max value of S / \sqrt{B} .

cat1: $-0.4 < \text{BDT-score} < 0.55$

Multivariate Analysis Selection

- MVA: ggH category

- Training results:

FIX! possible to add cat0 and cat1 lines?

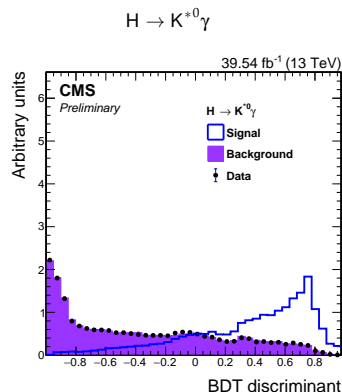
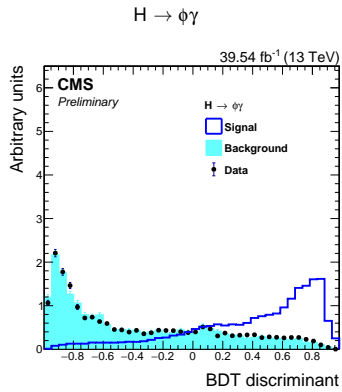
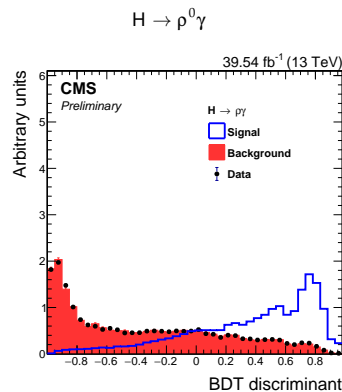


Figure 8: BDT-score shown for the three decay channels of ggH.

Multivariate Analysis Selection

- MVA: High & Low- p_T^γ VBF categories

- Training samples

Signal: MC-generated

Background: γ +jets simulation and γ di-track events where the two tracks have the same charge.

- 7 input variables

Variable that is correlated with Higgs candidate mass is divided by the mass.

FIX! does not match with paper!

$p_T^{\text{M}\gamma}$	Higgs candidate p_T
p_T^γ	photon p_T
$p_T^{\text{M}} / m_{\text{M}\gamma}$	meson p_T divided by Higgs candidate mass
$I^{\text{trk}}(\text{trk}_1)$	leading-track charged isolation
M_{jj}	di-jet invariant mass
$\Delta\phi_{jj}$	$\Delta\phi$ of the two jets
z^*	Zeppenfeld variable

- BDT sub-categories

cat0: BDT-score > 0.7 , optimized for max value of S/\sqrt{B} .

cat1: $-0.6 < \text{BDT-score} < 0.7$

Multivariate Analysis Selection

- **MVA: High- p_T^γ category**

- Training results:

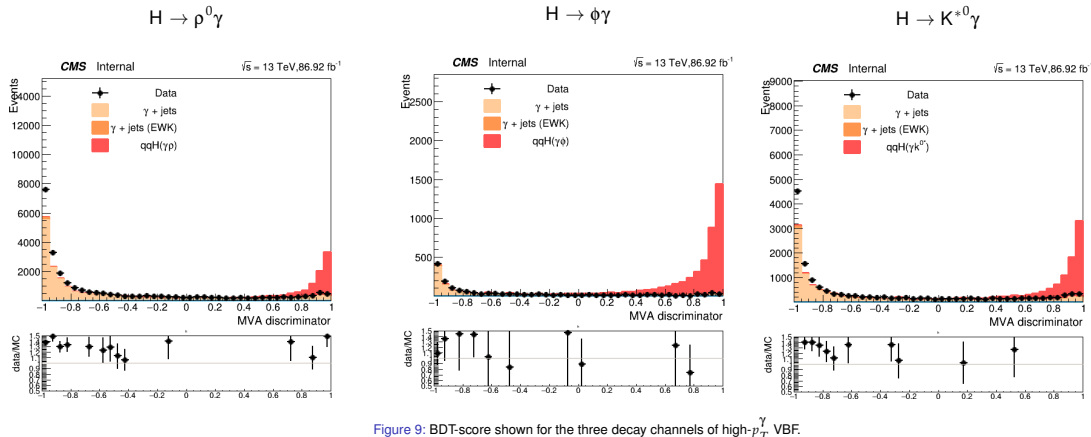


Figure 9: BDT-score shown for the three decay channels of high- p_T^γ VBF.

Multivariate Analysis Selection

- **MVA: Low- p_T^γ category**

- Training results:

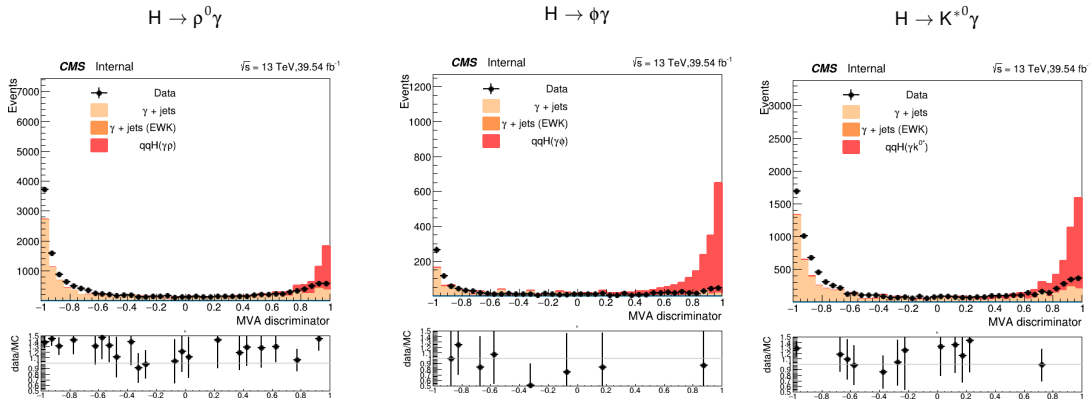


Figure 10: BDT-score shown for the three decay channels of low- p_T^γ VBF.

Signal & Background Modeling

Signal modeling

- Signal events extracted from the distribution of the **reconstructed Higgs boson mass**.
- Analytic function: **two-tailed Crystal Ball(TTCB)**.

$$\text{TTCB}(t) = \begin{cases} e^{-t^2/2}, & \text{for } -\alpha_L < t < \alpha_R \\ (\frac{n_L}{|\alpha_L|})^{n_L} e^{-\alpha_L^2/2} (\frac{n_L}{|\alpha_L|} - |\alpha_L| - t)^{-n_L}, & \text{for } t \leq -\alpha_L \\ (\frac{n_R}{|\alpha_R|})^{n_R} e^{-\alpha_R^2/2} (\frac{n_R}{|\alpha_R|} - |\alpha_R| + t)^{-n_R}, & \text{for } t \geq \alpha_L \end{cases}$$

- Fitted via unbinned likelihood to simulated signal events.

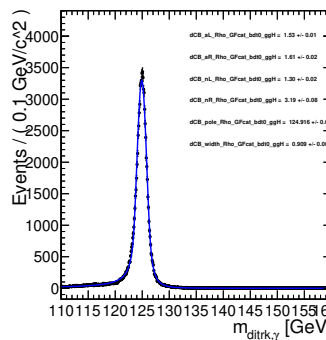


Figure 11: Example fitting of the TTCB function to the $H \rightarrow \rho^0 \gamma$ selected signal samples from BDT cat0 in the ggH category.

Background modeling

- Analytic functions: **Chebychev** polynomials (main), **Bernstein** polynomials and **exponential** series (determination of shape uncertainties).
- Fitting region defined as $m_{M\gamma}$ sidebands.
 - ggH category: $110 < m_{M\gamma} < 120$ GeV & $130 < m_{M\gamma} < 160$ GeV.
 - VBF categories (high & low p_T^γ): $100 < m_{M\gamma} < 120$ GeV & $130 < m_{M\gamma} < 170$ GeV.
 - VH category: $100 < m_{M\gamma} < 120$ GeV & $130 < m_{M\gamma} < 150$ GeV.
- Degree of polynomial determined with **F-test**.
- **Bias test**.

Systematic Uncertainties

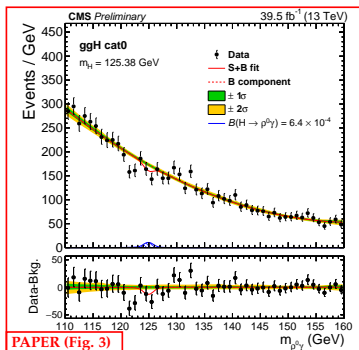
Systematic Uncertainties

Integrated Luminosity	2.5% (2016), 2.3% (2017), and 2.5% (2018)
Total inelastic cross section	4.6%
Trigger efficiencies	VBF-dedicated trigger, 2.2-3.4% (photon-leg) and 5.3-5.6% (di-jet)
Photon ID efficiencies	Up to 1.5%, p_T and η dependent
Tracking efficiency	4.6-4.8% (2.3-2.6% FIX! ?? per track)
Muon/Electron ID	Less than 1.0% (muons) / 1.5% (electrons)
Meson Charged/Neutral Isolation Efficiencies	1.7-2.8 %, depending on search channel and isolation type
JEC & JES	Up to 3.5% in VBF, negligible in ggH
QCD renormalization and factorization	0.4% (VBF), 0.7% (WH), 3.8% (ZH), and 2.6% (t <bar>t>H)</bar>
PDF & ff_S	1.6-3.2%, depending on Higgs production
Parton shower modeling	FIX! what is the number?

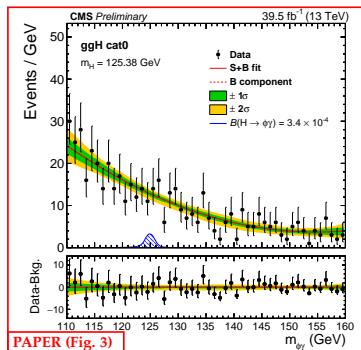
Results

Signal & Background Post-fit Distributions

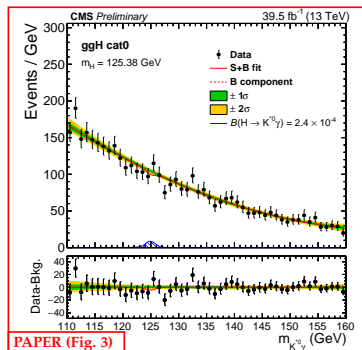
- ggH categories



$H \rightarrow \rho^0\gamma$, ggH cat0



$H \rightarrow \phi\gamma$, ggH cat0

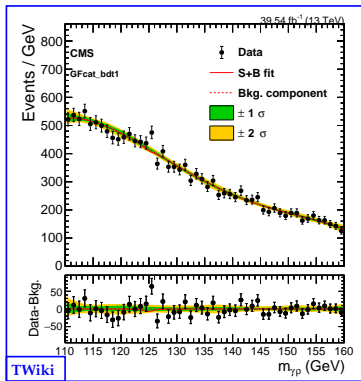


$H \rightarrow K^{*0}\gamma$, ggH cat0

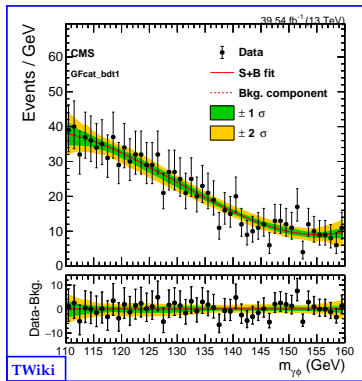
Figure 12: Post-fit $m_{M\gamma}$ distributions in data and the background model for the ggH cat0 channels.

Signal & Background Post-fit Distributions

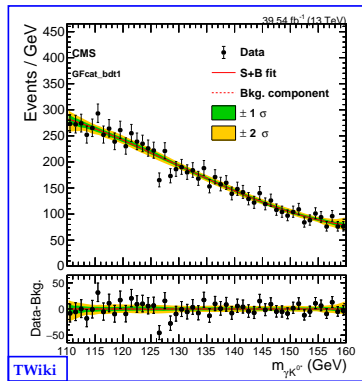
- ggH categories



$H \rightarrow \rho^0\gamma$, ggH cat1



$H \rightarrow \phi\gamma$, ggH cat1

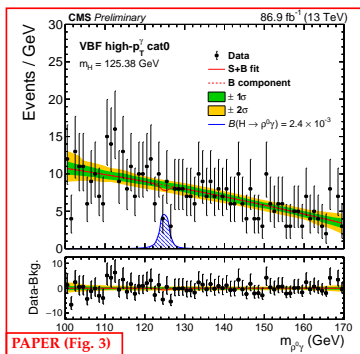


$H \rightarrow K^*\gamma$, ggH cat1

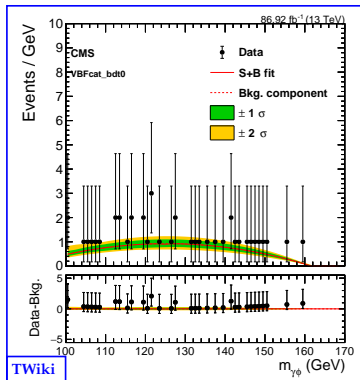
Figure 13: Post-fit $m_{M\gamma}$ distributions in data and the background model for the ggH cat1 channels.

Signal & Background Post-fit Distributions

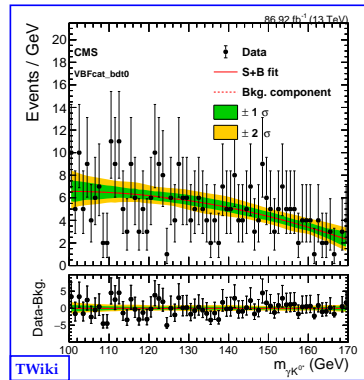
- High- p_T^γ VBF categories



$H \rightarrow p^0\gamma, \text{high-}p_T^\gamma \text{ VBF cat0}$



$H \rightarrow \phi\gamma, \text{high-}p_T^\gamma \text{ VBF cat0}$

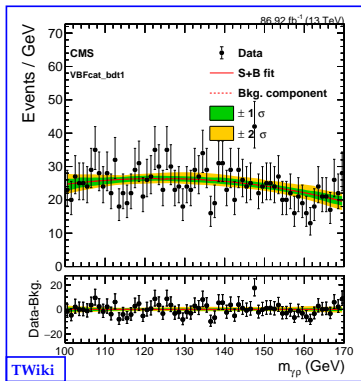


$H \rightarrow K^{*0}\gamma, \text{high-}p_T^\gamma \text{ VBF cat0}$

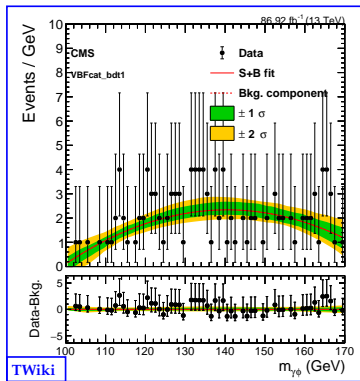
Figure 14: Post-fit $m_{M\gamma}$ distributions in data and the background model for the high- p_T^γ VBF cat0 channels.

Signal & Background Post-fit Distributions

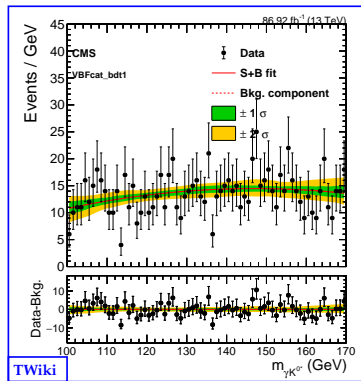
- High- p_T^γ VBF categories



$H \rightarrow \rho^0 \gamma$, high- p_T^γ VBF cat1



$H \rightarrow \phi \gamma$, high- p_T^γ VBF cat1

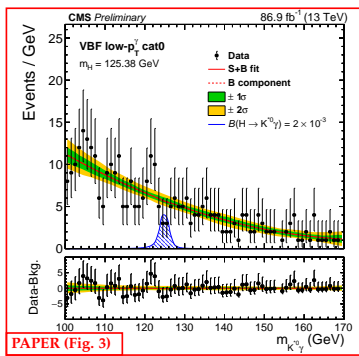


$H \rightarrow K^{*0} \gamma$, high- p_T^γ VBF cat1

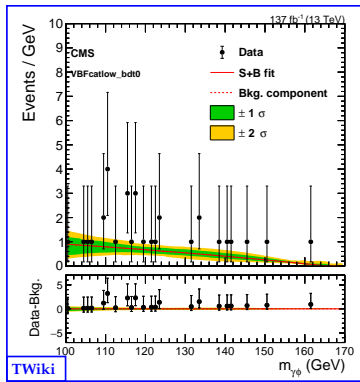
Figure 15: Post-fit $m_{M\gamma}$ distributions in data and the background model for the high- p_T^γ cat1 channels.

Signal & Background Post-fit Distributions

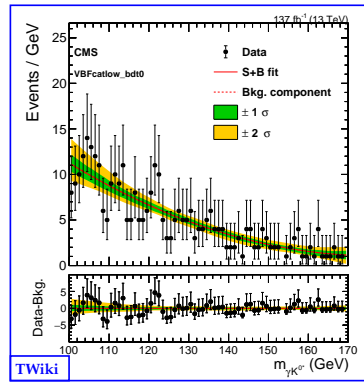
- Low- p_T^γ VBF categories



$H \rightarrow p^0 \gamma$, low- p_T^γ VBF cat0



$H \rightarrow \phi \gamma$, low- p_T^γ VBF cat0

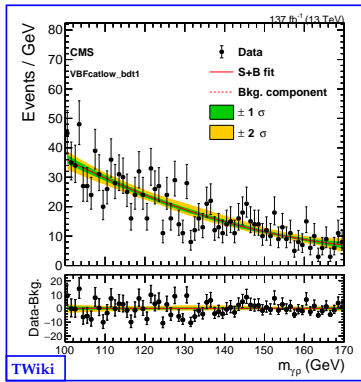


$H \rightarrow K^{*0} \gamma$, low- p_T^γ VBF cat0

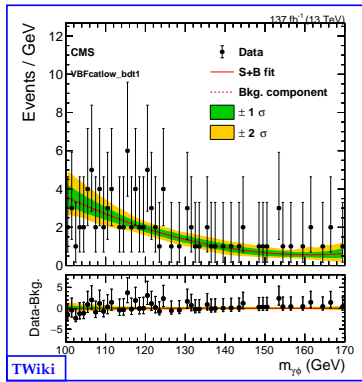
Figure 16: Post-fit m_{M_γ} distributions in data and the background model for the low- p_T^γ VBF cat0 channels.

Signal & Background Post-fit Distributions

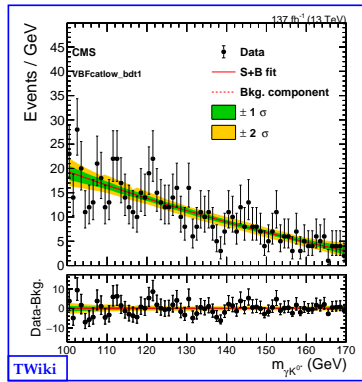
- Low- p_T^γ VBF categories



$H \rightarrow p^0\gamma$, low- p_T^γ VBF cat1



$H \rightarrow \phi\gamma$, low- p_T^γ VBF cat1

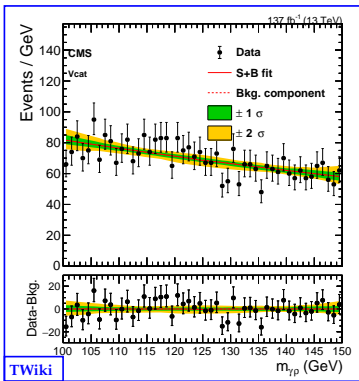


$H \rightarrow K^{*0}\gamma$, low- p_T^γ VBF cat1

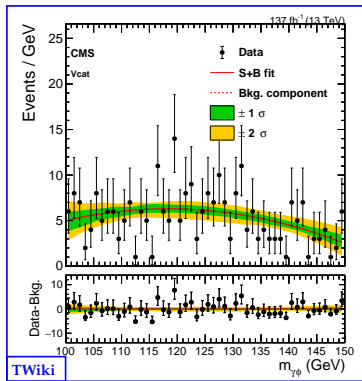
Figure 17: Post-fit m_{M_γ} distributions in data and the background model for the low- p_T^γ cat1 channels.

Signal & Background Post-fit Distributions

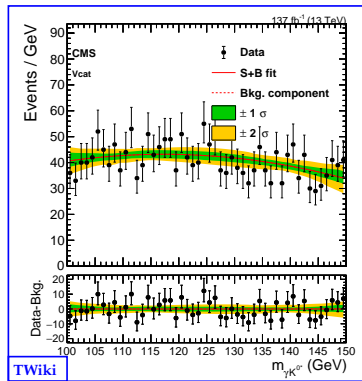
- VH categories



$H \rightarrow \rho^0 \gamma, \text{VH}$



$H \rightarrow \phi \gamma, \text{VH}$



$H \rightarrow K^{*0} \gamma, \text{VH}$

Figure 18: Post-fit $m_{M\gamma}$ distributions in data and the background model for the VH channels.

Upper Limits

- **Upper limits** on $\mathcal{B}(H \rightarrow \rho^0\gamma)$, $\mathcal{B}(H \rightarrow \phi\gamma)$, and $\mathcal{B}(H \rightarrow K^{*0}\gamma)$ set at 95% CL.
- CLs profile-likelihood ratio used as test-statistics, with the asymptotic approximation.
- Systematic uncertainties treated as nuisance parameters.

Upper Limits

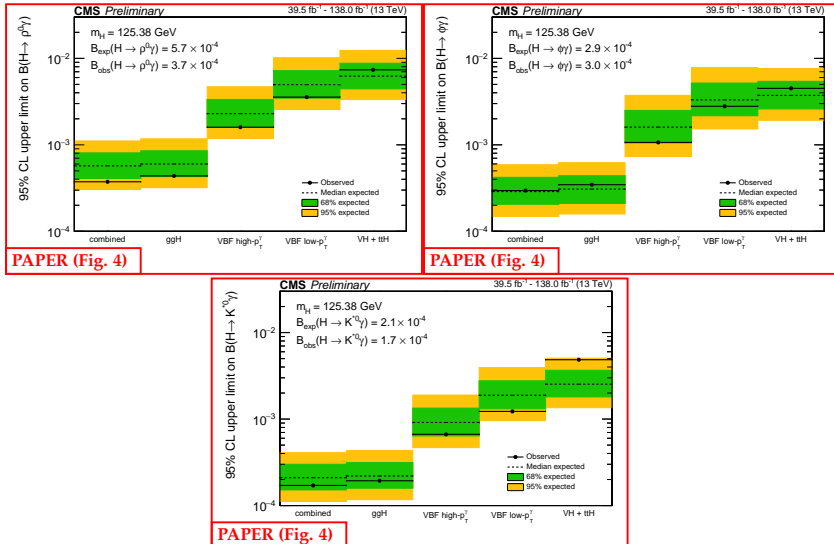


Figure 19: Expected and observed upper limits on $B(H \rightarrow \rho^0 \gamma)$ (top left), $B(H \rightarrow \phi \gamma)$ (top right), and $B(H \rightarrow K_0^* \gamma)$ (bottom) split by analysis categories and combined. Green and yellow bands correspond to 1 and 2σ confidence intervals in the expected upper limits.

Results

	U.L. $\mathcal{B}(H \rightarrow \rho^0 \gamma)$		U.L. $\mathcal{B}(H \rightarrow \phi \gamma)$		U.L. $\mathcal{B}(H \rightarrow K^{*0} \gamma)$	
category	Exp. (10^{-4})	Obs. (10^{-4})	Exp. (10^{-4})	Obs. (10^{-4})	Exp. (10^{-4})	Obs. (10^{-4})
VH	$62.3^{+25.6}_{-17.9}$	73.7	$37.3^{+16.9}_{-11.3}$	45.0	$25.3^{+11.4}_{-7.3}$	48.5
low- p_T^γ VBF	$49.6^{+22.5}_{-15.0}$	35.6	$33.1^{+18.7}_{-11.5}$	27.9	$18.8^{+8.90}_{-5.7}$	12.3
high- p_T^γ VBF	$22.9^{+10.5}_{-6.9}$	16.0	$16.0^{+9.0}_{-5.5}$	10.7	$9.13^{+4.25}_{-2.75}$	6.66
ggH	$6.01^{+2.53}_{-1.72}$	4.37	$3.08^{+1.33}_{-0.98}$	3.46	$2.20^{+0.94}_{-0.62}$	1.93
combined	$5.71^{+2.37}_{-1.63}$	3.74	$2.88^{+1.33}_{-0.83}$	2.97	$2.10^{+0.90}_{-0.58}$	1.71

PAPER (Table 2)

Figure 20: Exclusion limits at 95% CL on the branching fractions of the H boson decays. Observed and median expected limits with the upper and lower bounds in the expected 68% CL intervals are reported.

Results Comparison

Channel	Coupling	SM $\mathcal{BR}(H \rightarrow M\gamma)$	ATLAS Limits (10^{-4})	Our Limits (10^{-4})
$H \rightarrow \phi\gamma$	s	$(1.68 \pm 0.08) \times 10^{-5}$ [1]	Exp. $4.2^{+1.8}_{-1.2}$ Obs. 5.0 [5]	Exp. $2.88^{+1.33}_{-0.83}$ Obs. 2.97
$H \rightarrow \rho^0\gamma$	u, d	$(2.31 \pm 0.11) \times 10^{-6}$ [1]	Exp. $10.0^{+4.9}_{-2.8}$ Obs. 10.4 [5]	Exp. $5.71^{+2.37}_{-1.63}$ Obs. 3.74
$H \rightarrow K^{*0}\gamma$	$d\&s$ (flavor-changing)	(Only available for $H \rightarrow d\bar{s} + \bar{d}s$) 1.19×10^{-11} [2]	Exp. $3.7^{+1.5}_{-1.0}$ Obs. 2.2 [6]	Exp. $2.10^{+0.90}_{-0.58}$ Obs. 1.71

Table 6: Comparison of branching ratios obtained from theory, ATLAS, and this analysis.

Backup Slides

References

- [1] M. König and M. Neubert, "Exclusive radiative Higgs decays as probes of light-quark Yukawa couplings", *Journal of High Energy Physics* **2015** (2015) .
- [2] J.I. Aranda, G. González-Estrada, J. Montaño et al., "Revisiting the rare $H \rightarrow q_i q_j$ decays in the standard model", *Journal of Physics G: Nuclear and Particle Physics* **47** (2020) 125001.
- [3] CMS collaboration, "Electron and photon reconstruction and identification with the CMS experiment at the CERN LHC", *Journal of Instrumentation* **16** (2021) P05014.
- [4] A. Hoecker, P. Speckmayer, J. Stelzer et al., "TMVA - Toolkit for Multivariate Data Analysis", 2009.
- [5] ATLAS collaboration, "Erratum to: Search for exclusive Higgs and Z boson decays to $\phi\gamma$ and $\rho\gamma$ with the ATLAS detector", *Journal of High Energy Physics* **2023** (2023) .
- [6] ATLAS collaboration, "Search for exclusive Higgs and Z boson decays to $\omega\gamma$ and Higgs boson decays to $K_0^*\gamma$ with the ATLAS detector", *Physics Letters B* **847** (2023) 138292.